

# Comb and Dendrigraft Polystyrenes with Ferrocenyl Units at the Periphery: Synthesis and Electrochemical Properties

Julien Bernard,<sup>†</sup> Michel Schappacher,<sup>†</sup> Elio Ammannati,<sup>‡</sup> Alexander Kuhn,<sup>‡</sup> and Alain Deffieux\*,<sup>†</sup>

Laboratoire de Chimie des Polymères Organiques, UMR 5629 CNRS-ENSCP-Université Bordeaux 1, 16 Avenue Pey Berland, 33607 Pessac, France; and Laboratoire d'Analyse Chimique par Reconnaissance Moléculaire, ENSCPB, 16 Avenue Pey Berland, 33607 Pessac, France

Received June 21, 2002; Revised Manuscript Received September 17, 2002

**ABSTRACT:** Polystyrene (PS) combs and dendrigrafts bearing di(hydroxymethyl) group termini at each branch end were used as starting materials for the preparation of branched and hyperbranched polymer structures with ferrocenyl moieties at their periphery. Quantitative acetalization of the 1,3-propanol ends using carboxaldehyde ferrocene yields polymers with one ferrocenyl moiety per branch terminus. By varying the size of the different macromolecular building blocks used in the preparation of the hyperbranched polymers, in particular the  $\overline{DP}_n$  of the PS blocks forming the external branches, a series of ferrocenyl-functionalized polystyrene combs and dendrigrafts was prepared. Their electrochemical properties were studied by cyclic voltammetry in organic solution and compared with the corresponding  $\alpha$ -functional linear PS. Results show that all ferrocenyl groups in dendrigrafts are available and participate to the oxidation–reduction cycles while only a small fraction of the ferrocene groups is active in combs and linear PS.

## Introduction

As already shown for dendrimers,<sup>1–2</sup> the introduction of functional groups in the core or at the periphery of hyperbranched molecules is of great interest for potential applications in various fields of chemistry, biochemistry, and physics. In that context, the preparation and study of dendrimers containing organometallic complexes has recently received great attention,<sup>3,4</sup> and several groups have investigated in particular the introduction of ferrocenyl groups as redox-active moieties. Cuadrado et al. have synthesized silicon- and amine-based ferrocenyl containing dendrimers<sup>5–11</sup> with up to 64 ferrocenyl terminal units; the ferrocenyl units were reported to behave either as electronically communicating or noncommunicating redox centers depending on the dendrimer structure. The preparation of dendrimers with ferrocenyl end groups was also described by Astruc,<sup>12–15</sup> who studied their redox properties in solution and showed that these large molecules exhibit very stable activities. An investigation of the electrochemical properties of phosphorus-based dendrimers bearing ferrocenyl sensors located either in the core, within the branches, or at the periphery has been recently reported,<sup>16–17</sup> showing two distinct oxidation waves for the ferrocenyl units located in the inner and outer dendrimer layers, in agreement with different electronic environment.

The preparation and use of hyperbranched polymer structures as molecular support for functional groups or organometallic complexes is also of major interest and may represent an interesting alternative to the use of dendrimers. To our knowledge, ferrocene moieties have been incorporated in various polymer structures<sup>18–21</sup> but not directly on hyperbranched polymers. We reported recently a relatively easy route to the synthesis of

monodisperse PS combs and dendrigrafts with well-controlled chain characteristics (molar masses, low polymolecularity, number and size of branches, and functionality).<sup>22–26</sup> These hyperbranched macromolecular architectures resemble to molecular dendrimers although they have a less perfect structure. The large number of branches that characterizes these macromolecules, up to several thousands in the case of dendrigrafts, may allow as for dendrimers the introduction of a high number of terminal functions at their periphery. Indeed peripherically functionalized PS combs and dendrigrafts bearing functional organic groups at each branch terminus were very recently prepared in our group, following the route described in Scheme 1.<sup>27</sup> It may be anticipated that the location of the functional groups at the extremity of polymer branches that act as macromolecular spacer will favor their accessibility to reagents. This should also give to the anchored functions a quite uniform reactivity and behavior, with limited influence of groups attached to neighboring macromolecule branches.

In the present study, polystyrene combs and dendrigrafts with a di(hydroxymethyl) group at each branch end and the corresponding  $\alpha$ -functional linear PS chains were used as starting materials for the preparation of polymers bearing ferrocenyl moieties at their periphery. Functionalization by acetalization of the 1,3-propanol ends with carboxaldehyde ferrocene is first investigated. The electrochemical properties of different series of ferrocenyl-functionalized linear, comb, and dendrigraft polystyrene studied by cyclic voltammetry are then reported and data are correlated to the chain dimensions and architecture.

## Experimental Section

**Materials.** Ferrocene carboxaldehyde (98%, Sigma-Aldrich Chimie, Saint Quentin Fallavier, France) and tetrabutylammonium hexafluorophosphate, Bu<sub>4</sub>NPF<sub>6</sub>, (98%, Sigma Aldrich Chimie, Steinheim, Germany) were used as received.

<sup>†</sup> UMR 5629 CNRS-ENSCP-Université Bordeaux 1.

<sup>‡</sup> Laboratoire d'Analyse Chimique par Reconnaissance Moléculaire, ENSCPB.



gives 0.9 ferrocenyl unit per PS branch. No significant change in the apparent molar mass and molar distribution of the functionalized polymer ( $\bar{M}_{n,app} = 3.6 \times 10^5 \text{ g mol}^{-1}$ ,  $\bar{M}_w/\bar{M}_n = 1.06$ ), was observed by SEC analysis during this process. Similar experimental conditions and procedures were used for the preparation of ferrocenyl-functionalized linear PS and dendrigrafts. Note that the proton chemical shifts observed for the ferrocenyl units attached at chain-end of linear polystyrene ( $\delta = 4.13 \text{ ppm}$  (2H),  $\delta = 4.18 \text{ ppm}$  (5H), and  $\delta = 4.31 \text{ ppm}$  (2H)) are different from those observed from those attached to combs and dendrigrafts.

**Polymer Characterization.** SEC measurements were performed in THF at 20 °C (flow rate 0.7 mL/min) on a Varian apparatus equipped with refractive index (Varian) and laser light scattering (Wyatt Technology) dual detection and fitted with four TSK gel HXL columns with respectively 250, 1500,  $10^4$ , and  $10^5 \text{ Å}$  pore sizes and 5  $\mu\text{m}$  as bead size. Calibration in the case of refractive index detection was performed using linear polystyrene. For light scattering detection,  $dn/dc$  values of the graft copolymers were first determined in THF, with a laser source operating at 633 nm. Radii of gyration were determined by static light scattering.

$^1\text{H}$  NMR spectra were recorded on a BRUKER AC 200 MHz in  $\text{CDCl}_3$  at 25 °C.

Dynamic light scattering measurements ( $R_h$  and  $D$ ) were performed on a MALVERN apparatus (Zetasizer 3000 HS) equipped with a He–Ne laser source (633 nm). Correlation functions were analyzed by the Contin method. Latex particles were used as calibration standards.

MALDI–TOF spectra were recorded on a micromass TOF–STEC apparatus (Manchester, U.K.). The instrument is equipped with a pulsed  $\text{N}_2$  laser (337 nm, 4 ns pulse width) and time-delayed extracted ion source. Spectra were recorded in the positive-ion mode using the reflectron mode and with an accelerating voltage of 20 kV. Polymer samples were dissolved in THF at 10 mg/mL. The dithranol matrix solution was prepared by dissolving 10 mg in 1 mL of THF and the solution of cationization agent by dissolving NaI in MeOH. The solutions were combined in a 10:1:1 volume ratio of matrix to polymer to cationization agent. One to two microliters of the obtained solution was deposited onto the sample target and air-dried.

Cyclic voltammetry (CV) experiments were carried out in a conventional one compartment cell with a BAS 100B potentiostat at ambient temperature ( $20 \pm 2 \text{ °C}$ ) in freshly distilled THF solution containing 0.1 M  $\text{Bu}_4\text{NPF}_6$  supporting electrolyte that had been bubbled with nitrogen for at least 10 min. A 2 mm diameter gold or glassy carbon disk was used as the working electrode (EGG), and potentials were measured with respect to a commercial  $\text{Ag}|\text{AgCl}|3 \text{ M KCl}$  reference electrode (BAS). The counter electrode was a platinum wire. If not otherwise mentioned, scans were started at the positive end of the potential range.

## Results and Discussion

The new synthetic route we recently developed for the preparation of well-defined hyperbranched hydrocarbon polymers—combs and dendrigrafts—was adapted to the preparation of the corresponding peripherally functionalized hyperbranched macromolecules as illustrated in Scheme 1. The assembling process that is based on the efficient grafting of living anionic PSLi chains onto reactive poly(chloroethyl vinyl ether) backbones of various chain architectures was used to introduce in the last building step end-functional PS grafts prepared from protected functional anionic initiators, i.e. isopropylidene-2,2-di(hydroxymethyl)-1-(1-lithiobutoxy)butane in the present study. After the deprotection step, hyperbranched macromolecules with a dihydroxymethyl group at each branch end were obtained and used as molecular support for ferrocenyl groups. The SEC chromatograms of one linear PS, one comb, and one dendrigraft bearing

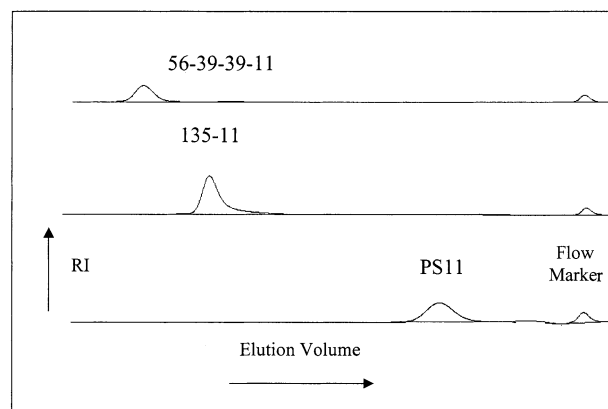


**Figure 1.** SEC chromatograms in THF at 20 °C of dihydroxymethyl-functionalized PS used as precursor for the preparation of ferrocene functionalized polymer architectures: linear PS ( $\text{DP}_n = 11$ ), comb PS (with  $\text{DP}_n = 135$  and 11 for the PCEVE backbone and PS branch), and dendrigraft polystyrene ( $\text{DP}_n = 60, 39, 39$  and 11, respectively, for the PCEVE backbone, the first PS block, the second PCEVE block, and the external PS branch).

dihydroxymethyl terminus and used as starting materials are shown in Figure 1.

**Synthesis of the Ferrocenyl-Functionalized Linear PS, Combs, and Dendrigrafts.** Acetalization of  $\alpha$ -dihydroxymethyl-functionalized polystyrenes was carried out with ferrocenyl carboxaldehyde as described in Scheme 2. This reaction is expected to yield macromolecules with one ferrocenyl moiety per linear chain, or per polymer branch in the case of branched and hyperbranched architectures. The grafting reaction of ferrocenyl moieties onto  $\alpha$ -dihydroxymethyl chain ends was first investigated in some detail in the case of linear polystyrene oligomers ( $\text{DP}_n = 40$ ). In methylene dichloride at 20 °C, in the presence of an acidic Amberlyst resin as catalyst and a 2-fold excess of ferrocene carboxaldehyde with respect to the  $\alpha$ -dihydroxymethyl PS terminus, the reaction is complete in about 12 h. The NMR spectrum and peak assignment of a functionalized PS oligomer ( $\text{DP}_n = 40$  denoted Fc40) is presented in Figure 2. Integration of the proton signals of ferrocene groups and PS units gives a functionality of 0.9 ferrocene per branch. The MALDI–TOF spectrum of the same PS oligomer (see Supporting Information) is in agreement with the calculated MALDI–TOF mass number ( $M = 386 + 104.15n$ ) for a ferrocenyl-functionalized PS with an  $\text{Fe}^+$  cation. The second peak series of  $\Delta m = +23$  corresponds to the sodium salt  $\text{Fc40} + \text{Na}^+$ . No noticeable trace of unfunctionalized PS oligomer is observed on the spectrum. Although polystyrenes linked to one ferrocene might be more easily cationized than unfunctionalized ones, these results are in line with NMR data and confirm the efficient end-functionalization of the PS chains by a ferrocenyl moieties. The characteristics of the linear FcPS series are collected in Table 1.

Similar experimental reaction conditions and procedures were then applied to the end-functionalization by a ferrocenyl group of PS branches of combs and dendrigrafts. The typical  $^1\text{H}$  NMR spectrum of a PS comb is presented in Figure 3. It is worthy noting that in the NMR spectra of Fc combs (as well as that of dendrigrafts), the chemical shifts of the ferrocenyl protons are, in particular, significantly different from those observed in linear FcPS (Figure 2). This may be attributed to the

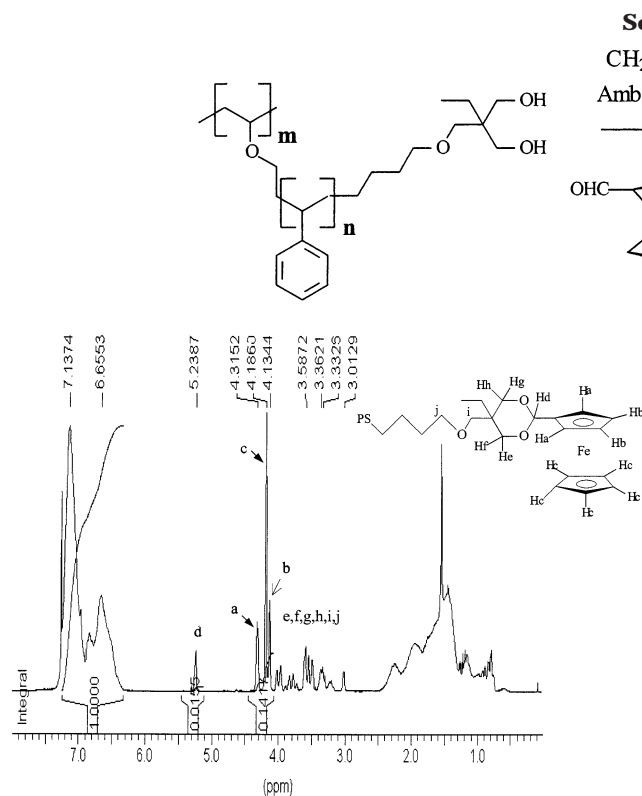


**Figure 2.** 200 MHz  $^1\text{H}$  NMR and peak assignment of a ferrocenyl-functionalized linear polystyrene, Fc40, in  $\text{CDCl}_3$ .

**Table 1. Dimensions, Diffusion Coefficient, and Electrochemical Properties of Ferrocenyl-Functionalized Linear Polystyrenes (Fc-PS) of Various  $\overline{\text{DP}}_n$**

sample reference	Fc <sup>a</sup>	Fc11 <sup>b</sup>	Fc40	Fc70	Fc110
$\overline{M}_n$ SEC		1150	4200	7000	11 500
$\overline{M}_w/\overline{M}_n$			1.03	1.06	1.08
exptl no. of Fc per PS chain <sup>c</sup>	1	0.88	0.83	0.9	0.9
diffusion coeff ( $\times 10^{-6} \text{ cm}^2 \text{ s}^{-1}$ )	7.3	6.2 <sup>d</sup>	3.2 <sup>d</sup>	2.3 <sup>d</sup>	1.8 <sup>d</sup>
exptl no. of redox-active Fc per PS chain <sup>e</sup>		n.d.	0.56	0.47	0.19
capacity <sup>f</sup> (mol/g) $\times 10^{-4}$		8.7	2.1	1.2	0.7

<sup>a</sup> Ferrocene:  $M = 186 \text{ g/mol}$ . <sup>b</sup> Refers to the PS  $\overline{\text{DP}}_n$  in the FcPS. <sup>c</sup> Calculated from the integration ratio between styrene aromatic protons (5H)/ferrocenyl protons (9H) and the  $\overline{\text{DP}}_n$  of the PS chain. <sup>d</sup> Diffusion coefficient of PS oligomers determined from the relation:  $D_{zo} = (3.0 \pm 0.4) \times 10^{-4} M_w^{-0.549 \pm 0.013}$ . <sup>e</sup> Determined from the relation of Randles-Sevcik:  $I_p = (2.69 \times 10^5) n^{3/2} A D^{1/2} \nu^{1/2} C$ . <sup>f</sup> Number of function per gram of polymer.

presence of different environments for the ferrocene in linear and branched polystyrenes. The average number of ferrocenyl units per PS branch estimated from the proton integration ratio between ferrocenyl and styrene units was found equal or higher than 0.9 per branch. Data are collected in Tables 2 and 3, for combs and dendrigrafts, respectively. The polymer functionality and capacity corresponding respectively to the number of ferrocenyl groups per polymer and per gram of polymer are also indicated for the different PS architectures. Depending on the chain topology, the size and the number of branches of the macromolecules, the number of ferrocenyl units varies from around 120 to 750 and approximately 1400–2000 in the comb and dendrigraft series, respectively. In the case of dendrigrafts, the resulting hyperbranched macromolecules present a typical core-shell structure with the redox-active ferrocenyl groups located in the shell.

It is worth noting that the solubility in organic solvents of the linear and branched FcPS structures are not noticeably modified after the functionalization step and all the polymers remained fully soluble in the conventional PS organic solvents.

**Electrochemical Study of Ferrocenyl-Functionalized PS.** The influence of the polymer dimensions and architecture on the electrochemical response of the attached ferrocenyl units was investigated by cyclic voltammetry. One could expect that, depending on the polymer structure and on their average distance within the molecule, ferrocenyl groups behave as isolated species or exhibit some form of mutual interaction. The increasing size and complexity of the molecular support should therefore have an impact on the electrochemical response of the ferrocenyl units.

A first and quite evident alteration of the electrochemical signal of the ferrocenyl moieties should come from the varying diffusion coefficients. As illustrated in Table 1 for a series of linear Fc-PS, the diffusion coefficient in THF decreases with increasing molar mass. Going from Fc40 to Fc110 yields a decrease by a factor 1.7. Indeed, the diffusion coefficients are significantly smaller than the literature value reported for ferrocene.<sup>29</sup> The peak currents in a cyclic voltammogram<sup>30</sup> can be theoretically evaluated from the Randles-Sevcik equation  $I_p = (2.69 \times 10^5) n^{3/2} A D^{1/2} \nu^{1/2} C$  (with  $I_p$  as peak current,  $n$  the number of electrons transferred per molecule,  $A$  the electrode surface,  $D$  the diffusion coefficient,  $\nu$  the scan rate, and  $C$  the concentration of ferrocenyl units). According to a calculation based solely on the varying diffusion coefficients, one should expect a decrease of approximately a factor 1.3 when comparing Fc40 and Fc110, keeping all other parameters constant. However, experimental data show a decrease by a factor of more than 6 in peak current when performing cyclic voltammograms in 0.1 mM solutions of the polymers in 0.1 M  $\text{Bu}_4\text{NPF}_6/\text{THF}$  (see Figure 4). The most likely interpretation is that for increasing chain lengths the ferrocenyl units are more and more wrapped in the polymer coil, and electron transfer with the electrode surface becomes more difficult. This results in a lower quantity of electrons transferred per time unit (current) as well as a broadening of the peaks and a larger separation between the oxidation and the reduction peaks, around 100 mV compared to the theoretically expected 56 mV.

Using the above equation one can calculate from the measured currents that statistically only 56% of the Fc40 molecules hitting the electrode participate in the electron transfer, whereas with the longer Fc110 this value even goes down to 19% (see Table 1).

For comblike PS architectures, the effect is still more pronounced. As can be seen from Table 2, the diffusion coefficient decreases not only when increasing the length of the branch where the ferrocene is attached but



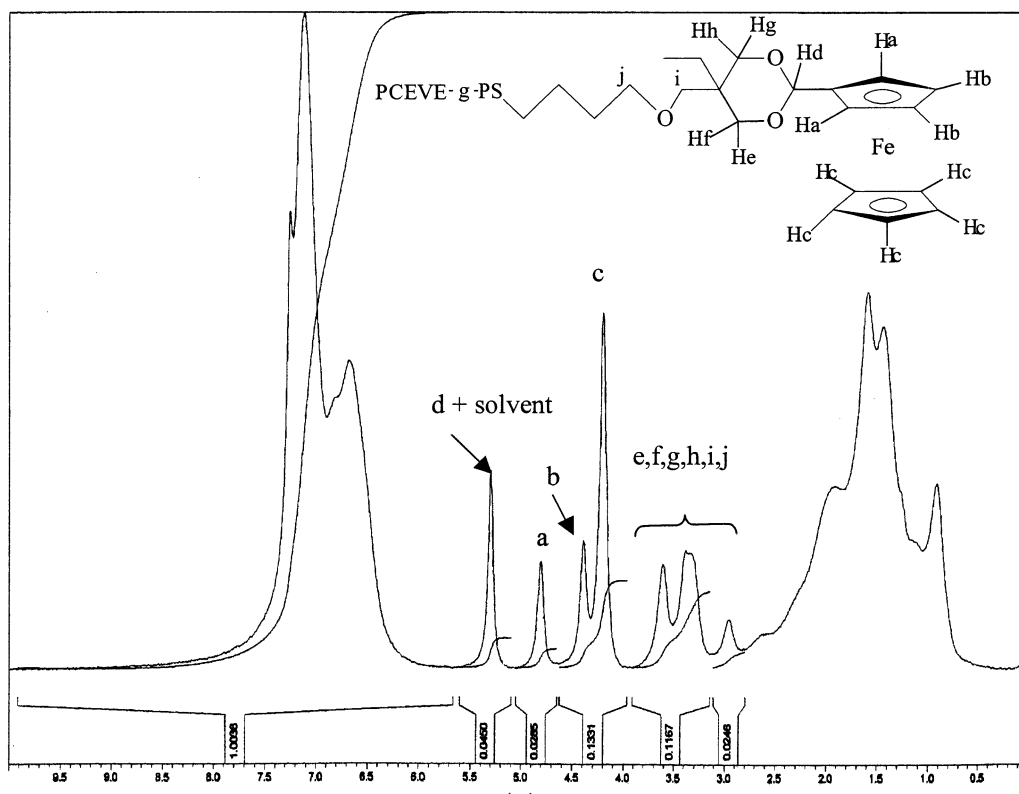


**Figure 3.** 200 MHz  $^1\text{H}$  NMR and peak assignment of a 760-Fc11 comb polystyrene in  $\text{CDCl}_3$ .

**Table 2. Dimensions, Diffusion Coefficient, and Electrochemical Properties of Ferrocenyl-Functionalized Comb Polystyrenes (PCEVE-FcPS) with Various Chain Parameters**

sample reference	135-Fc11 <sup>a</sup>	135-Fc40	135-Fc60	760-Fc11	760-Fc40	760-Fc60
exptl no. of branches/macromolecule <sup>b</sup>	135	133	132	760	760	737
$R_h^c$ (nm)	n.d.	16	16.2	n.d.	24	36
av Fc functionality per PS branch <sup>d</sup>	$\geq 0.9$	$\geq 0.9$	$\geq 0.9$	$\geq 0.9$	$\geq 0.9$	$\geq 0.9$
min no. of ferrocenes per macromolecule <sup>e</sup>	122	120	119	760	684	663
diffusion coeff <sup>c</sup> ( $\times 10^{-6} \text{ cm}^2 \text{ s}^{-1}$ )	n.d.	0.36	0.29	n.d.	0.20	0.13
exptl no. (and percentage) of redox-active Fc per macromolecule <sup>g</sup>	n.d. <sup>f</sup>	58 (48%)	33 (28%)	n.d. <sup>f</sup>	116 (17%)	$\sim 0$
capacity <sup>h</sup> (mol/g) $\times 10^{-4}$	7.8	2.1	1.4	7.8	2.1	1.4

<sup>a</sup> Indicates the respective  $\overline{\text{DP}}_n$  of the PCEVE backbone and of the PS branch. <sup>b</sup> See ref 25. <sup>c</sup> Determined by dynamic light scattering. <sup>d</sup> Calculated from the integration ratio between styrene aromatic protons (5H)/ferrocenyl protons (9H) and the  $\overline{\text{DP}}_n$  of the PS branch. <sup>e</sup> Experimental number of branches  $\times$  average functionality of a branch. <sup>f</sup> Not calculated because of adsorption phenomena. <sup>g</sup> Determined from the relation of Randles-Sevcik:  $I_p = (2.69 \times 10^5) n^{3/2} A D^{1/2} \nu^{1/2} C$ . <sup>h</sup> Number of Fc functions per gram of polymer.

**Table 3. Dimensions, Diffusion Coefficient, and Electrochemical Properties of Ferrocenyl-Functionalized Dendrigrift Polystyrenes (PCEVE-PS-PCEVE-FcPS) with Various Chain Parameters**

sample reference	56-39-39-Fc11 <sup>a</sup>	56-39-39-Fc40	56-39-39-Fc60
experimental no. of branches per macromolecule <sup>b</sup>	2108	1660	1567
$R_h^c$ (nm)	20	22	34
av functionality <sup>d</sup> per external branch	$\geq 0.9$	$\geq 0.9$	$\geq 0.9$
no. of functions per macromolecule <sup>e</sup>	1897	1494	1410
diffusion coeff <sup>c</sup> ( $\times 10^{-6} \text{ cm}^2 \text{ s}^{-1}$ )	0.23	0.21	0.14
exptl no. (and percentage) of redox-active Fc per macromolecule <sup>g</sup>	n.d. <sup>f</sup>	1494 (100%)	1410 (100%)
capacity <sup>h</sup> (mol/g) $\times 10^{-4}$	7.8	2.1	1.4

<sup>a</sup> Indicates the respective  $\overline{\text{DP}}_n$ s of the first PCEVE backbone, first PS block, second PCEVE block and external Fc-PS branches. <sup>b</sup> See ref 25. <sup>c</sup> Determined by dynamic light scattering. <sup>d</sup> Calculated from the integration ratio between styrene aromatic protons (5H)/ferrocenyl protons (9H) and the  $\overline{\text{DP}}_n$  of the external PS branch. <sup>e</sup> Experimental number of branches  $\times$  average functionality of a branch. <sup>f</sup> Not calculated because of the adsorption phenomenon. <sup>g</sup> Determined from the relation of Randles-Sevcik:  $I_p = (2.69 \times 10^5) n^{3/2} A D^{1/2} \nu^{1/2} C$ . <sup>h</sup> Number of functions per gram of polymer.

also when increasing the backbone  $\overline{\text{DP}}_n$  is observed. Solutions of the different PS prepared with an equal overall concentration of ferrocenyl units give a weaker and weaker electrochemical response. This effect is illustrated in Figure 5 where two combs with lateral chains of equal length but different backbones are compared. Although their diffusion coefficients measured by light scattering only differ by a factor of 1.8,

the electrochemical response is approximately six times smaller for the 760-Fc40 comb than for 135-Fc40 one. In the former case the diffusion coefficient is around forty times smaller than the one for ferrocene ( $7.3 \times 10^{-6} \text{ cm}^2 \text{ s}^{-1}$ ),<sup>27</sup> and therefore, the measured peak current by definition should be only about six times lower than that of a ferrocene molecule. Indeed, it is 80 times smaller. This is likely because the ferrocenyl

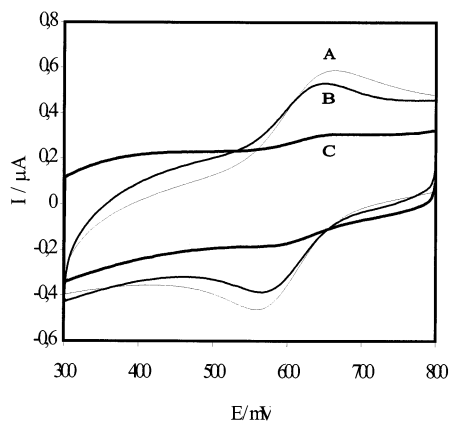


**Figure 4.** Cyclic voltammograms at 200 mV/s of linear Fc-PS with various chain lengths. Each compound is present at a concentration of 0.1 mM in 0.1 M Bu<sub>4</sub>NPF<sub>6</sub>/THF supporting electrolyte. Key: (A) Fc40; (B) Fc70; (C) Fc110.

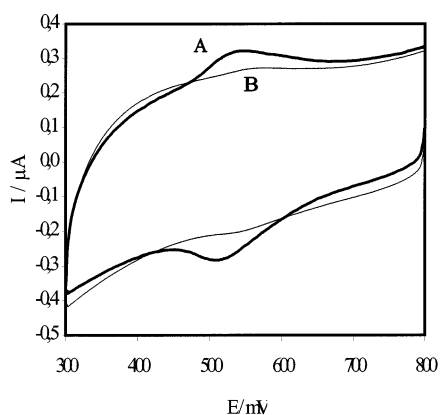


**Figure 5.** Cyclic voltammograms at 200 mV/s of two comblike polymers with different backbone length in 0.1 M Bu<sub>4</sub>NPF<sub>6</sub>/THF supporting electrolyte. The ferrocenyl concentration is 0.1 mM. Key: (A) 135-Fc40; (B) 760-Fc40.

moieties, although anchored at the extremity of the comb branches, are more and more buried in the polymer and therefore their electronic accessibility is highly reduced. One can easily calculate that statistically only 17% of the ferrocenes present in one comb polymer molecule participate in the electron transfer reaction, which obviously is a severe drawback for practical applications. An additional feature that is important to mention at this point is the increasing adsorption on the electrode surface for the more ramified PS molecules. This gives rise to a more complex peak pattern than for the above-mentioned linear PS. The adsorbed species and those freely diffusing in the electrolyte both contribute to the electrochemical signal, and therefore, especially for some PS combs (760-Fc11 and 135-Fc11), it was not possible to perform such a type of electrochemical analysis. Even for the other examined PS species (except the linear ones), the voltammograms contain a contribution from adsorption phenomena and therefore the obtained values for the experimental number of redoxactive ferrocene units per molecule (see Tables 2 and 3) are affected by a more or less large experimental error. Nevertheless, these values are still reliable enough to reflect the global trend concerning the accessibility of the redox units. In some cases, especially when changing the electrode material, the observed adsorption is strong enough to prepare stable modified electrodes, for example when using glassy carbon as a substrate.

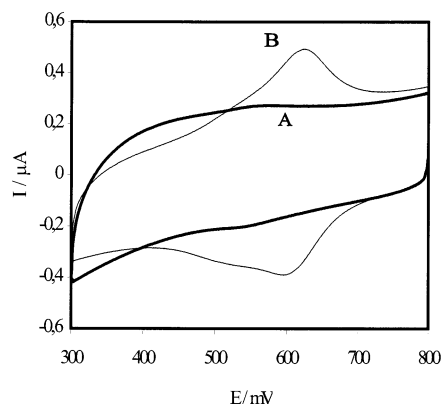


**Figure 6.** Cyclic voltammograms at 200 mV/s of a comblike polymer (760-Fc40) (curve A) and a PS dendrigrift (56-39-39-Fc40) (curve B), with 0.1 mM ferrocenyl substituents in 0.1 M Bu<sub>4</sub>NPF<sub>6</sub>/THF as supporting electrolyte.

Changing the macromolecular architecture and using dendrigrifts instead of comblike PS can circumvent the above-mentioned disadvantage of generating only partially electroactive ferrocenyl moieties. Despite the very high molar mass of dendrigrifts compared to PS combs, the experimental diffusion coefficients do not decrease further but even slightly grow; see Tables 2 and 3. Comparing for example the 760-Fc40 comb ( $\bar{M}_w = 3.5 \times 10^6$ ) and the 56-39-39-Fc40 dendrigrift ( $\bar{M}_w = 9.4 \times 10^6$ ) with approximately the same diffusion coefficient, one can explain this result by the values of the hydrodynamic radius and/or the radius of gyration of the two species: the two values are smaller for the dendrigrift molecule ( $R_h = 22.3$  nm;  $R_g = 20$  nm) than for the comb macromolecule ( $R_h = 24$  nm;  $R_g = 38$  nm). However, this alone cannot explain the better electrochemical response of the dendrigrifts. In fact when renormalizing the peak current measured for the dendrigrift by the reduced diffusion coefficient with respect to the ferrocene molecule, one can calculate that all the ferrocene units in a given hyperbranched macromolecule participate in the electron-transfer reaction. In the illustrated example (56-39-39-Fc40), this means that approximately 2000 electrons can be transferred from every macromolecule arriving at the electrode. However, the signal is again perturbed by adsorption, and in general, it is difficult or impossible for this large molecules to observe a pure diffusion current (see Figure 6). A similar problem has been pointed out already for large dendrimer molecules.<sup>12</sup> Nevertheless, the difference between both combs and dendrigrifts is evident at least from a qualitative point of view. Globally the same concentration of ferrocene substituents is present in both solutions, but the architecture of the macromolecular support on which they are packed is crucial for the accessibility in terms of electron transfer. For the globular structures, experimental data suggest that the ferrocenes are exposed at the outer sphere whereas in the case of comblike structures as well as for linear PS the polymer chain shields most of the redox units.

Shielding seems to be less important when the macromolecules are adsorbed at the electrode/electrolyte interface. Using comblike molecules with short side chains, a quite stable adsorption can be obtained on glassy carbon as illustrated in Figure 7. An interesting feature is the gradual increase of adsorbed material as a function of the number of potential cycles. Most likely the molecules become more hydrophilic during oxidation of the ferrocene units and therefore leave the organic

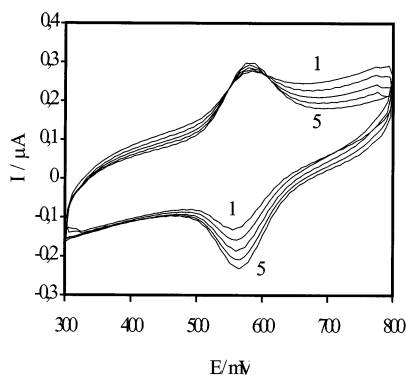


**Figure 7.** Adsorption of a comblike polymer (760-Fc11) on glassy carbon: first five successive potential cycles (200 mV/s) in a solution containing 0.2 mM ferrocenyl substituents in 0.1 M  $\text{Bu}_4\text{NPF}_6/\text{THF}$ , indicating a steady accumulation of polymer at the electrode-solution interface.

supporting electrolyte in order to interact with the electrode surface. The peak separation is less than 10 mV, which indicates the presence of an adsorbed species, and the peak width at half-height is very close to the theoretically expected 90 mV for a monoelectronic wave.<sup>30</sup> This means that all ferrocene units in one macromolecule have the same redox potential, or in other words, the individual ferrocenes are so far from one another that there is no mutual interaction and therefore they behave as independent redox centers. This is a quite expected behavior for these compounds because of the location of each ferrocene at the end of a macromolecular spacer. This also agrees with the behavior observed in higher generation ferrocenyl dendrimers for which no interactions between the redox centers have been observed.<sup>9</sup>

The possibility to prepare stable modified electrodes with these compounds that show an almost ideal electrochemical reversibility opens up various possibilities of applications for example in the field of electrocatalysis. In particular, the opportunity to control the number of immobilized ferrocene groups on different levels by changing the structure of the polymer and accumulating a variable amount of modification layers by choosing an adequate number of potential cycles is a quite unique feature of these compounds. Furthermore, the reported hyperbranched macromolecular supports are not limited to ferrocene but can be easily used for the anchoring of other functional groups and work in this direction is underway in our laboratories.

## Conclusion

Linear polystyrene chains, polystyrene combs, and dendrigrafts with ferrocene end groups were prepared and their electrochemical behaviors compared. A variation of chain length and overall size greatly affects the diffusion coefficients of the molecules and the accessibility of their electroactive groups. Quantitative measurements have been performed to estimate the number of redox-active ferrocenes per macromolecule. Although these estimates are in some cases difficult to obtain because of overlapping contributions from freely diffusing and adsorbed species a general trend is clearly observed. Linear and comblike polystyrene shows an increased shielding of the ferrocenyl moieties with growing chain size, most likely because the macromolecule is more and more wrapped around the redox center. In contrast when going to more compact struc-

tures like the dendrigrafts, the ferrocene groups remain almost completely available for the electron exchange with the electrode, indicating that they must be located toward the outer side of these sphere like macromolecules. This opens up interesting possibilities in different fields like catalysis or redox mediation.

**Supporting Information Available:** Figure showing a MALDI-TOF chromatogram of a linear PS Fc40. This material is available free of charge via the internet at <http://pubs.acs.org>.

## References and Notes

- (1) Tomalia, D. A.; Esfand, R. *Chem. Ind.* **1997**, 11, 416.
- (2) Grubbs, R. B.; Hawker, C. J.; Dao, J.; Fréchet, J. M. J. *Angew. Chem., Int. Ed.* **1997**, 36, 270.
- (3) Newkome, G. R.; He, E.; Moorefield, C. N. *Chem. Rev.* **1999**, 99, 1689.
- (4) Oosterom, G. E.; Reek, J. N. H.; Kamer, P. C. J.; van Leeuwen, P. W. N. M. *Angew. Chem., Int. Ed.* **2001**, 40, 1828.
- (5) Takada, T.; Diaz, D. J.; Abruna, H. D.; Cuadrado, I.; Casado, C.; Alonso, B.; Moran, M.; Losada, J. *J. Am. Chem. Soc.* **1997**, 119, 10763.
- (6) Cuadrado, I.; Moran, M.; Casado, C.; Alonso, B.; Lobete, F.; Garcia, R.; Ibasate, M.; Losada, J. *Organometallics* **1996**, 15, 5278.
- (7) Cuadrado, I.; Casado, C.; Alonso, B.; Moran, M.; Losada, J.; Belsky, J. *J. Am. Chem. Soc.* **1997**, 119, 7613.
- (8) Losada, J.; Cuadrado, I.; Moran, M.; Casado, C.; Alonso, B.; Barranco, M. *Anal. Chim. Acta* **1997**, 338, 191.
- (9) Casado, C.; Cuadrado, I.; Moran, M.; Alonso, B.; Garcia, B.; Gonzalez, B.; Losada, J. *Coord. Chem. Rev.* **1999**, 185, 5–186, 53.
- (10) Casado, C.; Gonzalez, B.; Cuadrado, I.; Alonso, B.; Moran, M.; Losada, J. *Angew. Chem., Int. Ed.* **2000**, 39, 2135.
- (11) Castro, R.; Cuadrado, I.; Alonso, B.; Casado, C.; Moran, M.; Kaifer, A. E. *J. Am. Chem. Soc.* **1997**, 119, 5760.
- (12) Nlate, S.; Ruiz, J.; Sartor, V.; Navarro, R.; Blais, J. C.; Astruc, D. *Chem.-Eur. J.* **2000**, 6, 14.
- (13) Valerio, C.; Alonso, E.; Blais, J. C.; Astruc, D. *Angew. Chem., Int. Ed.* **1999**, 38, 12.
- (14) Valerio, C.; Alonso, E.; Blais, J. C.; Astruc, D. *Angew. Chem.* **1999**, 111, 11855.
- (15) Valerio, C.; Fillaut, J. L.; Ruiz, J.; Guittard, J.; Blais, J. C.; Astruc, D. *J. Am. Chem. Soc.* **1997**, 119, 2588.
- (16) Turrin, C. O.; Chiffre, J.; Daran, J. C.; De Montauzon, D.; Caminade, A. M.; Manoury, E.; Balavoine, G.; Majoral, J. P. *Macromolecules* **2000**, 33, 7328.
- (17) Turrin, C. O.; Chiffre, J.; Daran, J. C.; De Montauzon, D.; Caminade, A. M.; Manoury, E.; Balavoine, G.; Majoral, J. P. *Tetrahedron* **2001**, 57, 2521.
- (18) Saraceno, R. A.; Riding, G. H.; Allcock, H. R.; Ewing, A. E. *J. Am. Chem. Soc.* **1988**, 110, 7254.
- (19) Albagli, D.; Bazan, G.; Wrighton, M. S.; Schrock, R. R. *J. Am. Chem. Soc.* **1992**, 114, 4150.
- (20) Crumbliss, A. L.; Cooke, D.; Castillo, J.; Wisian-Neilson, P. *Inorg. Chem.* **1993**, 32, 6088.
- (21) Casado, C. M.; Moran, M.; Losada, J.; Cuadrado, I. *Inorg. Chem.* **1995**, 34, 1668.
- (22) Muchtar, Z.; Schappacher, M.; Deffieux, A. *Macromolecules* **2001**, 34, 7595.
- (23) Deffieux, A.; Schappacher, M. *Macromolecules* **1999**, 32, 1797.
- (24) Schappacher, M.; Billaud, C.; Paulo, C.; Deffieux, A. *Macromol. Chem. Phys.* **1999**, 200, 2377.
- (25) Schappacher, M.; Deffieux, A. *Macromol. Chem. Phys.* **1997**, 198, 3953.
- (26) Schappacher, M.; Muchtar, Z.; Bernard, J.; Deffieux, A. *Macromol. Symp.*, in press.
- (27) Schappacher, M.; Bernard, J.; Deffieux, A. Submitted for publication.
- (28) Schappacher, M.; Deffieux, A. *Macromolecules* **2001**, 34, 5827.
- (29) Amatore, C.; Azzabi, M.; Calas, P.; Jutand, A.; Lefrou, C.; Rollin, Y. *J. Electroanal. Chem.* **1990**, 288, 45.
- (30) Bard, A. J.; Faulkner, L. R. *Electrochemical Methods*; Wiley: New York, 1980.